

## 6-Acyl-4-aryl/alkyl-5,7-dihydroxycoumarins as anti-inflammatory agents

Chun-Mao Lin,<sup>a</sup> Sheng-Tung Huang,<sup>b</sup> Fu-Wei Lee,<sup>c</sup>  
Hsien-Saw Kuo<sup>a</sup> and Mei-Hsiang Lin<sup>a,\*</sup>

<sup>a</sup>Department of Biochemistry, Taipei Medical University, 250 Wu-Xing Street, Taipei 110, Taiwan, ROC

<sup>b</sup>Department of Chemical Engineering and Biotechnology, National Taipei University of Technology,  
Jhong-Xia E. Rd., Sec. 3, Taipei 106, Taiwan, ROC

<sup>c</sup>Graduate Institute of Medical Sciences, College of Medicine, Taipei Medical University,  
250 Wu-Xing Street, Taipei 110, Taiwan, ROC

Received 1 December 2005; revised 20 February 2006; accepted 21 February 2006

Available online 15 March 2006

**Abstract**—A series of coumarin derivatives were synthesized in two steps from phloroglucinol. The anti-inflammatory activities of these derivatives were evaluated by means of inhibiting NO production in LPS-induced RAW 264.7 cells. Derivatives **3**, **8**, **10**, **11**, and **13** exhibited low micromolar levels of anti-inflammatory activities, and these derivatives also protected DNA against hydroxyl radical attack. Coumarin derivative **8** was the most potent derivative among those tested herein against NO production in LPS-induced RAW 264.7 cells with an IC<sub>50</sub> value of 7.6 μM, and it effectively reduced the hydroxyl radical production by 50% at 100 μM in the electron spin resonance study.

© 2006 Elsevier Ltd. All rights reserved.

### 1. Introduction

The general chemical structure of coumarins consists of a benzene moiety fused to α-pyrone rings, and they are a class of phenolic substances commonly found in plants. Coumarin derivatives are known to possess multiple pharmacological activities, such as antiviral<sup>1</sup> and antitumor activities,<sup>2–6</sup> DNA-repair deficiencies,<sup>7,8</sup> and anti-inflammation.<sup>9–13</sup> For example, coumarin (**1**) was shown to reduce tissue edema and inflammation, and pharmacological studies revealed that it is an effective agent for reducing the formation of and scavenging of reactive oxygen species (ROS) involved in free radical-mediated injury.<sup>14,15</sup>

Nitric oxide (NO) production has been implicated in the process of carcinogenesis and inflammation. NO is released by a family of enzymes including constitutive NO synthase (cNOS) and an inducible NO synthase (iNOS). NO is also involved in the production of vascular endothelial growth factor (VEGF); the overex-

pression of NO has been shown to induce angiogenesis, vascular hyperpermeability, and accelerated tumor development.<sup>16</sup> iNOS-mediated excessive NO generation has been reported to cause mutagenesis and deamination of DNA bases and to form carcinogenic *N*-nitrosamine. Suppression of the biochemical pathway for the induction of NO or a reduction in the activities of iNOS is a new paradigm for the prevention of carcinogenesis and relief of inflammation in several organs. Thus, selective inhibitors of iNOS may have a therapeutic role in certain diseases.<sup>17</sup>

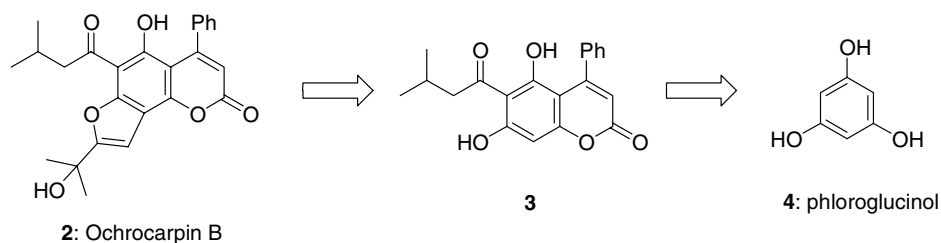
ROS have previously been viewed as general messengers for signal-induced nuclear factor kappa B (NF-κB) activation. It has been reported that suppression of ROS-mediated NO elevation might be beneficial in reducing the development of inflammation. Several studies have shown that antioxidant agents are able to reduce the occurrence of inflammation and cancer through decreasing the amount of oxidative stress, and prostaglandin and nitric oxide production in cells.<sup>18</sup>

Ochrocarpin B (**2**) represents a new class of coumarin analogues, isolated from the bark of *Ochrocarpos punctatus* H. Perrier (Clusiaceae). The structure of ochrocarpin B was assigned based on its physical

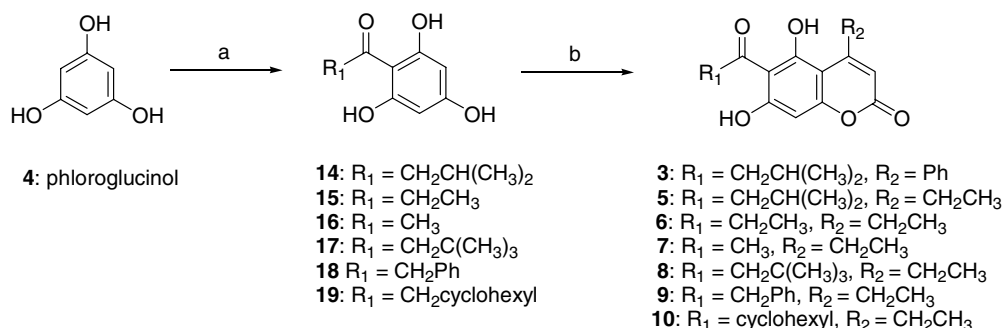
**Keywords:** iNOS; ROS; Anti-inflammation; Coumarin.

\* Corresponding author. Tel.: +886 2 27361661x3162; fax: +886 2 27361661x3164; e-mail: [mhl00001@tmu.edu.tw](mailto:mhl00001@tmu.edu.tw)

and spectral characteristics.<sup>19</sup> The architectural framework of **2** is a coumarin ring skeleton fused with a furan moiety at positions 7 and 8, and bears a hydroxyl group at position 5. Ochrocarpin B exhibited anticancer activity with an IC<sub>50</sub> value of 3.8 μg/mL against ovarian cancer cells.<sup>19</sup> We are in the process of working on the total synthesis of this natural product. During the progression of our total synthesis, one of the synthetic intermediates, **3**, which contains the core coumarin structure of ochrocarpin B, showed low micromolar levels of anti-inflammatory action by means of inhibition of NO production in lipopolysaccharide (LPS)-treated RAW 264.7 cells with an IC<sub>50</sub> value of 9.0 μM. This result sparked our interest to further examine the anti-inflammatory effects of the coumarin derivatives with a similar architectural framework to that of ochrocarpin B without the fused furan moiety, and we were especially interested in the derivatives with various substituents at positions 4 and 6 of the coumarin ring. In this study, we synthesized a series of 4,6-di-substituted coumarins (**5–10**), and evaluated their anti-inflammatory activities which occurred by means of inhibition of NO production in LPS-activated RAW 264.7 macrophage cells. Since scavenging of the hydroxyl radicals produced during inflammation is one mechanism that many anti-inflammatory agents possess as a means to suppress NO production, we were also interested in understanding the level of the hydroxyl radical-scavenging effect of our synthetic derivatives. We employed both DNA protection experiments and electron spin resonance (ESR) to demonstrate that our selective derivatives were also effective agents for scavenging hydroxyl radicals (Scheme 1).



Scheme 1.



**Scheme 2.** Reagents and Conditions: (a) isovaleryl chloride or properly acyl chloride, AlCl<sub>3</sub>, nitrobenzene, 60 °C, 40–70%; (b) ethyl benzoylacetate or ethyl propionyl acetate, rt, 12–42%.

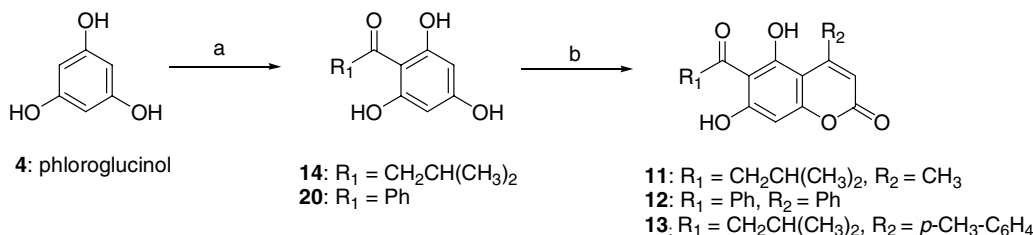
## 2. Results and discussion

### 2.1. Chemistry

Since various therapeutic applications of coumarins are known, many efforts have been made to synthesize the benzopyranone moiety, and the Pechmann reaction has frequently been employed to do this. In the Pechmann reaction, the precursor phenols condensed with β-keto esters in the presence of acid lead to formation of the benzopyranone moiety.<sup>20–22</sup> Thus, we also employed the Pechmann reaction as the means to prepare coumarin derivatives **3** and **5–13**, and the synthetic scheme is outlined in Scheme 2. The synthesis began with preparation of acylphloroglucinols (**14–20**). Mono-acylation of phloroglucinol with proper acyl chlorides produced acylphloroglucinols **14–19** in 40–70% yields.<sup>23–25</sup> The benzyopyranone moiety in coumarin derivatives **3** and **5–13** was prepared by the reaction of acylphloroglucinols (**14–20**) with either benzoyl acid ester or ethyl propionylacetate to obtain **3** and **5–10** in 12–42% yields (Scheme 2). Derivatives **11–13** were synthesized using the same approach as **3**, and the synthetic scheme is outlined in Scheme 3 (7–37%, two-step yields). The efficient two-step synthesis developed herein allows the rapid creation of a series of coumarin derivatives, that is, **3** and **5–13**, for evaluating anti-inflammatory activities.

### 2.2. Biological results

**2.2.1. Effects of chromen-2-ones (3 and 5–13) on the inhibition of NO production.** The overproduction of NO is a key biochemical event during inflammation. Many



**Scheme 3.** Reagents and conditions: (a) isovaleryl chloride or benzoyl chloride, AlCl<sub>3</sub>, nitrobenzene, 60 °C, 44–68%; (b) ethyl benzoacetate or ethyl acetoacetate, rt, 15–54%.

**Table 1.** IC<sub>50</sub> of chromen-2-ones (**3**, **5**–**13**) for NO production by LPS-activated RAW264.7 macrophage cells

Compound	3	5	6	7	8	9	10	11	12	13
IC <sub>50</sub> (μM)	9.0	14.5	63.8	21.2	7.6	19.1	13.0	9.3	26.0	12.1

anti-inflammatory agents are potent effectors for suppressing NO production *in vivo*. We analyzed nitrite production as an indicator of the NO released in LPS-activated macrophages. The nitrite concentrations in the culture media were measured with and without the synthetics **3** and **5**–**13** co-incubated with macrophages prior to LPS (50 ng/mL) activation. When LPS was administered to RAW 264.7 macrophages, NO production dramatically increased, and macrophages co-incubated with **3** and **5**–**13** prior to LPS activation showed reduced NO production in RAW 264.7 macrophages. The inhibitory concentrations of **3** and **5**–**13** required to produce 50% NO production in LPS-activated RAW 264.7 macrophage are listed in Table 1, and their IC<sub>50</sub> values ranged from 7.6 to 63.8 μM. The inhibition of NO production in RAW 264.7 cells by coumarin derivatives synthesized herein was not due to general cellular toxicity, and the cell viability was verified using the MTT assay (data not shown). The coumarins dissolved in DMSO did not interfere with the Griess reaction. Coumarin **8** was the most potent agent tested among those synthesized herein with an IC<sub>50</sub> value of 7.6 μM, while **6** was the least effective agent for reducing NO production with an IC<sub>50</sub> value of 63.8 μM. The substituents at position 6 of the coumarin derivatives exhibited influences on inhibiting NO production in RAW 264.7 cells. Derivatives with isovaleryl and *tert*-butylacetyl substituents (compounds **3**, **5**, **8**, **11**, and **13**) at position

**6** of the coumarin ring tended to have lower IC<sub>50</sub> values as compared with those of other substituents such as benzyl, propionyl, and acetyl. On the other hand, substituents at position 4 of the coumarin derivatives exhibited less influence on the inhibiting NO production in RAW 264.7 cells (Chart 1).

The iNOS protein expressions in LPS-activated macrophage cells with pretreated selective coumarin derivatives **3**, **8**, **10**, **11**, and **13** were also evaluated (Fig. 1). RAW 264.7 cells maintained under normal conditions expressed undetectable levels of iNOS protein (Fig. 1, lane 1). After stimulation with LPS, the amount of iNOS protein expressed increased (Fig. 1, lane 2). The LPS-activated macrophages co-incubated with coumarin derivatives **3**, **8**, **10**, **11**, and **13** displayed a reduction in iNOS protein expression (Fig. 1, lanes 3–7) as compared to LPS alone. The relative amounts of iNOS protein in macrophages co-incubated with equal amounts (15 μM) of compounds **3**, **8**, **10**, **11**, and **13** were 0.25, 0.57, 0.69, 0.76, and 0.80, respectively, versus LPS alone. The derivatives **3**, **8**, and **10** were the most effective agents among those tested for reducing iNOS expression.

**2.2.2. Effects of coumarins on protecting supercoiled DNA from hydroxyl radical damage.** Many known anti-inflammatory agents possess the abilities to scavenge hydroxyl

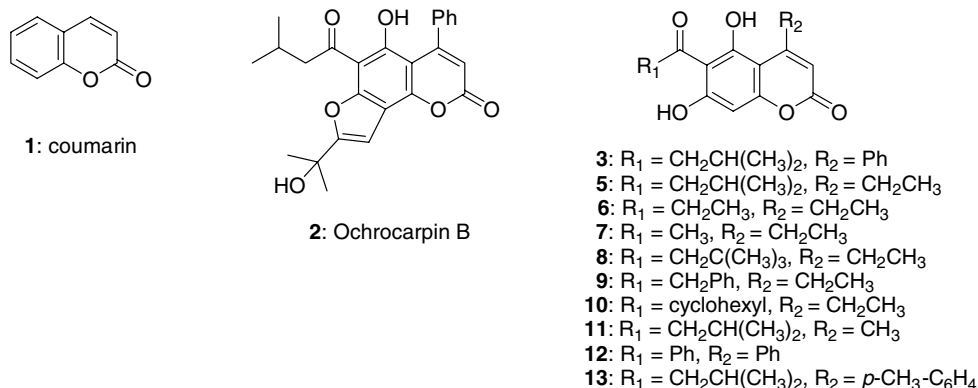


Chart 1.



breakage; therefore, it was chosen for this experiment. The results of ESR are shown in Figure 2B. In the absence of **8**, 2 mM of H<sub>2</sub>O<sub>2</sub> and 50 μM of FeSO<sub>4</sub> generated an electron spin resonance signal with a peak height of 98. Under the same conditions, the peak heights of electron spin resonance signals were reduced to 50 and 22 in the presence of 50 and 100 μM of compound **8**, respectively (Fig. 2B). This result suggests that **8** is an effective agent in competing with DMPO for hydroxyl radicals. This result combined with the results of the DNA protection experiment suggests that **8** is an effective hydroxyl radical scavenger. The anti-inflammatory effect induced by **8** may be correlated with its hydroxyl radical-scavenging ability.

### 3. Conclusions

In conclusion, a series of coumarins has been prepared as potential anti-inflammatory agents, and we have identified that the particle structural analogue of ochrocarpin B, **8**, is a potent agent for reducing NO production in LPS-activated macrophages. Furthermore, derivative **8** may be an effective agent in scavenging hydroxyl radicals produced during the process of inflammation. Further detailed molecular pharmacological studies examining derivative **8** are currently underway. We believe that the efficient synthesis approach disclosed herein can lead to the rapid output of a series of coumarins for evaluation and anti-inflammatory mechanism studies, and the anti-inflammatory mechanism study herein holds promise for the development of a new generation of potent anti-inflammatory agents.

## 4. Experimental procedures

### 4.1. General experimental conditions

Melting points were determined in a capillary tube using a MEL-TEMP II melting point apparatus by Laboratory Devices. NMR spectra were recorded on Bruker DMX-500 FT-NMR spectrometers; chemical shifts were recorded in parts per million downfield from Me<sub>4</sub>Si. IR spectra were determined with a Perkin-Elmer 1760-X FT-IR spectrometer. Mass spectra were recorded on Jeol JMS-D300 and FINNIGAN TSQ-46C mass spectrometers; HRMS was obtained with a Jeol JMS-HX110 spectrometer. TLC was performed on Merck (Art. 5715) silica gel plates and visualized under UV light (254 nm), upon treatment with iodine vapor, or upon heating after treatment with 5% phosphomolybdic acid in ethanol. Flash chromatography was performed with Merck (Art. 9385) 40–63 μm silica gel 60. Elemental analyses were carried out on a Perkin-Elmer 240 elemental analyzer, and the results were within ± 0.4% of the theoretical values.

### 4.2. Preparation of acylphloroglucinol

Aluminum trichloride (48 mmol) was added to a stirred suspension of anhydrous phloroglucinol (**4**, 12 mmol) in nitrobenzene (30 mL) and stirred for 30 min at room

temperature. Then acyl chloride (12 mmol) was injected and heated to 60 °C for 2 h, and the reaction mixture was cooled to room temperature. The mixture was poured onto ice water and extracted with ethyl acetate. The organic layer was extracted with 10% NaOH<sub>(aq)</sub> and the alkaline layer was neutralized with concentrated HCl followed by extraction with ethyl acetate. The ethyl acetate extract was washed with water and brine, dried (MgSO<sub>4</sub>), filtered, and evaporated. The residue was chromatographed (silica gel, EtOAc/*n*-hexane 1:5) to produce acylphloroglucinol as a solid.

**4.2.1. (3-Methylbutyryl)phloroglucinol (14).** Starting from isovaleryl chloride (5.0 mL, 40.0 mmol), **14** (5.7 g, 68%) was obtained as a yellow solid. <sup>1</sup>H NMR (500 MHz, DMSO-*d*<sub>6</sub>) δ 0.88 (s, 3H), 0.89 (s, 3H), 2.11 (m, 1H), 2.84 (d, *J* = 6.8 Hz, 2H), 5.78 (s, 2H), 10.33 (s, 1H), 12.23 (s, 2H); <sup>13</sup>C NMR (125 MHz, DMSO-*d*<sub>6</sub>) δ 22.48, 24.65, 48.56, 52.30, 127.16, 127.44, 128.02, 138.92, 158.91; MS (FAB) *m/z* 210 (MH<sup>+</sup>), 153 (base peak).

**4.2.2. 1-(2,4,6-Trihydroxy-phenyl)-propan-1-one (15).** Starting from propionyl chloride (1.06 mL, 11.9 mmol), **15** (1.2 g, 55%) was obtained as a yellow solid. <sup>1</sup>H NMR (500 MHz, DMSO-*d*<sub>6</sub>) δ 1.03 (t, 3H), 3.00 (q, 2H), 5.79 (s, 2H), 10.29 (s, 1H), 12.21 (s, 2H); <sup>13</sup>C NMR (125 MHz, DMSO-*d*<sub>6</sub>) δ 8.71, 36.40, 94.63, 103.66, 164.19, 164.44, 205.70; MS (FAB) *m/z* 183 (MH<sup>+</sup>, base).

**4.2.3. 2,4,6-Trihydroxy-acetophenone (16).** Starting from acetyl chloride (867 μL, 11.9 mmol), **16** (0.8 g, 40%) was obtained as a yellow solid. <sup>1</sup>H NMR (500 MHz, DMSO-*d*<sub>6</sub>) δ 2.53 (s, 3H), 5.78 (s, 2H), 10.36 (s, 1H), 12.22 (s, 2H); <sup>13</sup>C NMR (125 MHz, DMSO-*d*<sub>6</sub>) δ 94.43, 105.74, 128.04, 128.47, 131.81, 139.86, 159.40, 161.87, 196.52; MS (FAB) *m/z* 169 (MH<sup>+</sup>), 56 (base peak).

**4.2.4. 3,3-Dimethyl-1-(2,4,6-trihydroxy-phenyl)-butan-1-one (17).** Starting from *tert*-butylacetyl chloride (1.12 mL, 7.93 mmol), **17** (1.25 g, 70%) was obtained as a yellow solid. <sup>1</sup>H NMR (500 MHz, DMSO-*d*<sub>6</sub>) δ 0.98 (s, 9H), 2.99 (s, 2H), 5.77 (s, 2H), 10.32 (s, 1H), 12.25 (s, 2H); <sup>13</sup>C NMR (125 MHz, DMSO-*d*<sub>6</sub>) δ 94.43, 105.74, 128.04, 128.47, 131.81, 139.86, 159.40, 161.87, 196.52; MS (FAB) *m/z* 225 (MH<sup>+</sup>), 154 (base peak).

**4.2.5. 2,4,6-Trihydroxy-deoxybenzoin (18).** Starting from phenylacetyl chloride (1.59 mL, 11.9 mmol), **18** (1.14 g, 39%) was obtained as a yellow solid. <sup>1</sup>H NMR (500 MHz, DMSO-*d*<sub>6</sub>) δ 4.33 (s, 2H), 5.81 (s, 2H), 7.18–7.29 (m, 5H), 10.39 (s, 1H), 12.21 (s, 2H); <sup>13</sup>C NMR (125 MHz, DMSO-*d*<sub>6</sub>) δ 48.94, 94.71, 103.72, 126.22, 128.06, 129.67, 135.94, 164.27, 164.89, 202.33; MS (FAB) *m/z* 245 (MH<sup>+</sup>), 58 (base peak).

**4.2.6. 2-Cyclohexyl-1-(2,4,6-trihydroxy-phenyl)-ethanone (19).** Starting from cyclohexanecarboxylic acid chloride (543 μL, 3.96 mmol), **19** (0.4 g, 40%) was obtained as a yellow solid. <sup>1</sup>H NMR (500 MHz, DMSO-*d*<sub>6</sub>) δ 1.22–1.31 (m, 5H), 1.64 (d, *J* = 12.0 Hz, 1H), 1.74 (d, *J* = 9.3 Hz, 2H), 1.80 (d, *J* = 9.3 Hz, 2H), 3.57 (t, *J* = 2.7 Hz, 1H), 5.78 (s, 2H), 10.30 (s, 1H), 12.24 (s, 2H); <sup>13</sup>C NMR (125 MHz, DMSO-*d*<sub>6</sub>) δ 25.73, 29.12,



48.54, 59.78, 94.79, 103.06, 164.21 164.37, 208.40; MS (FAB)  $m/z$  237 ( $MH^+$ , base).

**4.2.7. 2,4,6-Trihydroxy-benzophenone (20).** Starting from benzoyl chloride (1.84 mL, 16 mmol), **20** (1.6 g, 44%) was obtained as a yellow solid.  $^1H$  NMR (500 MHz, DMSO- $d_6$ )  $\delta$  5.84 (s, 2H), 7.43 (t,  $J = 7.7$  Hz, 2H), 7.51 (t,  $J = 7.4$  Hz, 1H), 7.61 (d,  $J = 7.7$  Hz, 2H), 9.82 (s, 1H), 10.08 (s, 2H);  $^{13}C$  NMR (125 MHz, DMSO- $d_6$ )  $\delta$  94.43, 105.74, 128.04, 128.47, 131.81, 139.86, 159.40, 161.87, 196.52; MS (FAB)  $m/z$  231 ( $MH^+$ ), 154 (base peak).

### 4.3. Preparation of 6-acyl-5,7-dihydroxycoumarins

Concentrated  $H_2SO_4$  (0.2 mL) was added to a mixture of acylphloroglucinol (1 mmol) and benzoyl acid ester (1.1 mmol) in glacial HOAc (3 mL) and stirred for 2 h at room temperature. The precipitate was filtered, washed with water, and crystallized with MeOH to give the product.

**4.3.1. 5,7-Dihydroxy-6-(3-methyl-butyryl)-4-phenyl-chromen-2-one (3).** Starting from **14** (4.4 g, 20.9 mmol), **3** (0.83 g, 12%) was obtained as a canary-yellow solid. Mp: 253–255 °C;  $R_f$  0.50 ( $CH_2Cl_2/MeOH$  10:1); IR (neat) 3000–3500, 1689, 1616  $cm^{-1}$ ;  $^1H$  NMR (500 MHz, DMSO- $d_6$ )  $\delta$  0.89 (s, 3H), 0.90 (s, 3H), 2.11 (m, 1H), 2.95 (d,  $J = 6.5$  Hz, 2H), 5.84 (s, 1H), 6.37 (s, 1H), 7.31–7.33 (m, 2H), 7.37–7.39 (m, 3H);  $^{13}C$  NMR (125 MHz, DMSO- $d_6$ )  $\delta$  22.47, 24.62, 52.35, 94.70, 100.65, 106.49, 111.39, 127.15, 127.44, 128.04, 138.93, 155.56, 158.86, 159.61, 163.80, 164.68, 207.07; MS (EI, 70 eV)  $m/z$  338 ( $M^+$ ), 170 (base peak); HRMS (EI) calculated for  $C_{20}H_{18}O_5^+$ : 338.1149, found: 338.1154.

**4.3.2. 5,7-Dihydroxy-6-(3-methyl-butyryl)-4-ethyl-chromen-2-one (5).** Starting from **14** (0.2 g, 0.95 mmol), **5** (0.10 g, 36%) was obtained as a canary-yellow solid. Mp: 229–232 °C;  $R_f$  0.50 (EtOAc/ $n$ -hexane 1:1); IR (KBr) 3000–3500, 1686, 1616  $cm^{-1}$ ;  $^1H$  NMR (500 MHz, DMSO- $d_6$ )  $\delta$  0.92 (s, 3H), 0.93 (s, 3H), 1.16 (t,  $J = 7.4$  Hz, 3H), 2.17 (m, 1H), 2.94 (q,  $J = 7.2$  Hz, 3H), 2.98 (d,  $J = 6.9$  Hz, 2H), 5.94 (s, 1H), 6.29 (s, 1H), 11.97 (s, 1H), 15.53 (s, 1H);  $^{13}C$  NMR (125 MHz, DMSO- $d_6$ )  $\delta$  13.52, 22.53, 24.64, 28.47, 52.43, 94.78, 101.46, 106.41, 108.25, 159.24, 159.698, 160.10, 163.25, 165.35, 207.27; MS (EI, 70 eV)  $m/z$  290 ( $M^+$ ), 233 (base peak); HRMS (EI) calculated for  $C_{16}H_{18}O_5^+$ : 290.1149, found: 290.1162.

**4.3.3. 5,7-Dihydroxy-6-propyryl-4-ethyl-chromen-2-one (6).** Starting from **15** (0.25 g, 1.37 mmol), **6** (0.13 g, 36%) was obtained as a canary-yellow solid. Mp: 259–262 °C;  $R_f$  0.61 (EtOAc/ $n$ -hexane 1:1); IR (KBr) 3000–3500, 1678, 1624  $cm^{-1}$ ;  $^1H$  NMR (500 MHz, DMSO- $d_6$ )  $\delta$  1.08 (t,  $J = 7.0$  Hz, 3H), 1.16 (t,  $J = 7.3$  Hz, 3H), 2.93 (q,  $J = 7.3$  Hz, 3H), 3.13 (q,  $J = 7.0$  Hz, 2H), 5.93 (s, 1H), 6.30 (s, 1H), 11.9 (s, 1H), 15.5 (s, 1H);  $^{13}C$  NMR (125 MHz, DMSO- $d_6$ )  $\delta$  8.33, 13.5, 28.5, 37.2, 94.7, 101.4, 106.2, 108.3, 159.3, 159.6, 160.1, 163.4, 165.1, 208.2; MS (EI, 70 eV)  $m/z$  262 ( $M^+$ ), 233 (base peak); HRMS (EI) calculated for  $C_{14}H_{14}O_5^+$ : 262.0836, found: 262.0841.

**4.3.4. 5,7-Dihydroxy-6-acetyl-4-ethyl-chromen-2-one (7).** Starting from **16** (0.25 g, 1.50 mmol), **7** (0.13 g, 35%) was obtained as a canary-yellow solid. Mp: 257–260 °C;  $R_f$  0.38 ( $CH_2Cl_2/MeOH$  10:1); IR (KBr) 3000–3500, 1713, 1627  $cm^{-1}$ ;  $^1H$  NMR (500 MHz, DMSO- $d_6$ )  $\delta$  1.16 (t,  $J = 7.3$  Hz, 3H), 2.68 (s, 3H), 2.93 (q,  $J = 7.3$  Hz, 3H), 5.94 (s, 1H), 6.30 (s, 1H);  $^{13}C$  NMR (125 MHz, DMSO- $d_6$ )  $\delta$  13.5, 28.4, 33.0, 94.7, 101.3, 106.5, 108.3, 159.2, 159.9, 160.1, 163.6, 165.2, 205.2; MS (EI, 70 eV)  $m/z$  248 ( $M^+$ ), 205 (base peak); HRMS (EI) calculated for  $C_{14}H_{14}O_5^+$ : 248.0679, found: 248.0688.

**4.3.5. 6-(3,3-Dimethyl-butyryl)-5,7-dihydroxy-4-ethyl-chromen-2-one (8).** Starting from **17** (0.25 g, 1.11 mmol), **8** (0.65 g, 39%) was obtained as a canary-yellow solid. Mp: 231–234 °C;  $R_f$  0.38 ( $CH_2Cl_2/MeOH$  10:1); IR (KBr) 3000–3500, 1705, 1625  $cm^{-1}$ ;  $^1H$  NMR (500 MHz, DMSO- $d_6$ )  $\delta$  1.01 (s, 9H), 1.16 (t,  $J = 7.3$  Hz, 3H), 2.94 (q,  $J = 7.2$  Hz, 3H), 5.94 (s, 1H), 6.29 (s, 1H);  $^{13}C$  NMR (125 MHz, DMSO- $d_6$ )  $\delta$  13.6, 28.5, 29.7, 31.8, 54.1, 94.9, 101.5, 107.6, 159.3, 159.6, 160.1, 163.1, 165.1, 207.6; MS (EI, 70 eV)  $m/z$  304 ( $M^+$ ), 233 (base peak); HRMS (EI) calculated for  $C_{19}H_{16}O_5^+$ : 304.1305, found: 304.1311.

**4.3.6. 6-(Phenylacetyl)-5,7-dihydroxy-4-phenyl-chromen-2-one (9).** Starting from **18** (0.25 g, 1.03 mmol), **9** (0.14 g, 42%) was obtained as a yellow solid. Mp: 244–246 °C;  $R_f$  0.50 (EtOAc/ $n$ -hexane 1:1); IR (KBr) 3000–3500, 1690, 1620  $cm^{-1}$ ;  $^1H$  NMR (500 MHz, DMSO- $d_6$ )  $\delta$  1.15 (t,  $J = 7.2$  Hz, 3H), 2.93 (q,  $J = 7.2$  Hz, 3H), 5.95 (s, 1H), 6.33 (s, 1H), 7.23–7.32 (m, 5H), 12.1 (s, 1H), 15.3 (s, 1H);  $^{13}C$  NMR (125 MHz, DMSO- $d_6$ )  $\delta$  13.6, 49.7, 94.9, 101.5, 106.4, 108.4, 126.5, 128.2, 129.8, 135.0, 159.2, 159.9, 160.1, 163.3, 165.3, 205.1; MS (EI, 70 eV)  $m/z$  324 ( $M^+$ ), 233 (base peak); HRMS (EI) calculated for  $C_{19}H_{16}O_5^+$ : 324.0992, found: 324.1001.

**4.3.7. 6-(2-Cyclohexanoyl)-5,7-dihydroxy-4-ethyl-chromen-2-one (10).** Starting from **19** (0.31 g, 1.24 mmol), **10** (0.15 g, 34%) was obtained as a yellow solid. Mp: 233–235 °C;  $R_f$  0.38 ( $CH_2Cl_2/MeOH$  10:1); IR (KBr) 3000–3500, 1699, 1607  $cm^{-1}$ ;  $^1H$  NMR (500 MHz, DMSO- $d_6$ )  $\delta$  1.14–1.28 (m, 4H), 1.28–1.35 (m, 4H), 1.67 (d,  $J = 12.6$  Hz, 1H), 1.75–1.78 (m, 2H), 1.87 (d,  $J = 10.1$  Hz, 2H), 2.93 (q,  $J = 7.2$  Hz, 2H), 3.66 (m, 1H), 5.94 (s, 1H), 6.30 (s, 1H), 12.0 (s, 1H);  $^{13}C$  NMR (125 MHz, DMSO- $d_6$ )  $\delta$  13.6, 25.6, 25.6, 28.5, 29.0, 49.3, 94.9, 101.6, 105.7, 108.3, 159.3, 159.6, 160.1, 162.9, 165.6, 210.8; MS (EI, 70 eV)  $m/z$  316 ( $M^+$ ), 233 (base peak); HRMS (EI) calculated for  $C_{14}H_{14}O_5^+$ : 316.1305, found: 316.1308.

**4.3.8. 5,7-Dihydroxy-6-(3-methyl-butyryl)-4-methyl-chromen-2-one (11).** Starting from **14** (0.65 g, 3.11 mmol), **11** (0.46 g, 54%) was obtained as a canary-yellow solid. Mp: 272–2274 °C;  $R_f$  0.50 (EtOAc/ $n$ -hexane 1:1); IR (KBr) 3000–3500, 1678, 1611  $cm^{-1}$ ;  $^1H$  NMR (500 MHz, DMSO- $d_6$ )  $\delta$  0.91 (s, 3H), 0.93 (s, 3H), 2.16 (m, 1H), 2.51 (s, 3H), 2.98 (d,  $J = 7.0$  Hz, 2H), 5.96 (s, 1H), 6.27 (s, 1H), 11.97 (s, 1H), 15.53 (s, 1H);  $^{13}C$

NMR (125 MHz, CDCl<sub>3</sub>)  $\delta$  22.51, 23.52, 24.68, 52.42, 94.62, 102.17, 106.44, 109.87, 154.91, 159.00, 159.47, 163.31, 165.70, 207.24; MS (EI, 70 eV)  $m/z$  276 (M<sup>+</sup>), 170 (base peak); HRMS (EI) calculated for C<sub>15</sub>H<sub>16</sub>O<sub>5</sub><sup>+</sup>: 276.0992, found: 276.0998.

**4.3.9. 6-Benzoyl-5,7-dihydroxy-4-phenyl-chromen-2-one (12).** Starting from **20** (1.10 g, 4.80 mmol), **12** (0.23 g, 15%) was obtained as a yellow solid. Mp: 267–269 °C;  $R_f$  0.58 (CH<sub>2</sub>Cl<sub>2</sub>/MeOH 10:1); IR (KBr) 3000–3500, 1677, 1624 cm<sup>-1</sup>; <sup>1</sup>H NMR (500 MHz, DMSO-*d*<sub>6</sub>)  $\delta$  5.78 (s, 1H), 6.34 (s, 1H), 7.35–7.41 (m, 5H), 7.54 (t,  $J$  = 7.7 Hz, 2H), 7.66 (t,  $J$  = 7.3 Hz, 1H), 7.81 (d,  $J$  = 7.5 Hz, 2H), 10.51 (s, 1H), 10.75 (s, 1H); <sup>13</sup>C NMR (125 MHz, DMSO-*d*<sub>6</sub>)  $\delta$  99.3, 100.9, 107.8, 111.0, 127.8, 127.9, 128.4, 129.3, 134.2, 137.8, 139.9, 154.1, 156.5, 158.1, 159.4, 159.5, 193.0; MS (EI, 70 eV)  $m/z$  358 (M<sup>+</sup>), 357 (base peak); HRMS (EI) calculated for C<sub>12</sub>H<sub>11</sub>NO<sup>+</sup>: 358.0836, found: 358.0826.

**4.3.10. 5,7-Dihydroxy-6-(3-methyl-butyryl)-4-(*p*-methyl-phenyl)-chromen-2-one (13).** Starting from **14** (0.25 g, 1.19 mmol), **13** (0.1 g, 24%) was obtained as a canary-yellow solid. Mp: 253–255 °C;  $R_f$  0.57 (CH<sub>2</sub>Cl<sub>2</sub>/MeOH 10:1); IR (KBr) 3000–3500, 1686, 1612 cm<sup>-1</sup>; <sup>1</sup>H NMR (500 MHz, DMSO-*d*<sub>6</sub>)  $\delta$  0.89 (s, 3H), 0.90 (s, 3H), 2.10–2.15 (m, 1H), 2.34 (s, 3H), 2.95 (d,  $J$  = 6.5 Hz, 2H), 5.83 (s, 1H), 6.37 (s, 1H), 7.17–7.22 (m, 4H), 12.07 (s, 1H), 14.89 (s, 1H); <sup>13</sup>C NMR (125 MHz, DMSO-*d*<sub>6</sub>)  $\delta$  20.9, 22.5, 24.7, 52.4, 94.7, 100.7, 106.5, 111.3, 127.2, 128.1, 136.0, 137.5, 155.7, 158.9, 159.7, 163.7, 164.7, 207.1; MS (EI, 70 eV)  $m/z$  352 (M<sup>+</sup>), 295 (base peak); HRMS (EI) calculated for C<sub>20</sub>H<sub>18</sub>O<sub>5</sub><sup>+</sup>: 352.1305, found: 352.1299.

#### 4.4. Biological assay

**4.4.1. Determination of nitrite.** The nitrite accumulated in the culture medium was measured as an indicator of NO production according to the Griess reaction.<sup>26</sup> Cells were plated in 24-well culture plates and stimulated with LPS (50 ng/mL) in the presence or absence of various concentrations of AS extracts for 24 h. One hundred microliters of each media supernatant was mixed with 50  $\mu$ L of 1% sulfanilamide (in 5% phosphoric acid) and 50  $\mu$ L of 0.1% naphthylethylenediamine dihydrochloride (in dH<sub>2</sub>O) at room temperature. The absorbance at 550 nm was measured with a NaNO<sub>2</sub> serial dilution standard curve, and nitrite production was determined.

**4.4.2. Western blot analysis.** Cellular protein was prepared using Gold lysis buffer. Proteins at 30–50  $\mu$ g were separated on SDS-PAGE and electrotransferred to a polyvinylidene difluoride (PVDF) membrane (Immobilon<sup>P</sup>, Millipore, Bedford, MA, USA). The membrane was incubated with primary antibody at room temperature for 2 h and then incubated with horseradish peroxidase-conjugated secondary IgG antibody; the immunoreactive bands were visualized with enhanced chemiluminescent reagents (ECL, Amersham, Buckinghamshire, UK).<sup>27</sup> Data were quantified using a densitometer (Alpha Innotech IS-1000 Digital Imaging System, San Leandro, CA, USA).

**4.4.3. Protection of supercoiled DNA from strand breakage by the Fenton reaction.** The inhibitory effect of compounds on supercoiled DNA strand breakage caused by the Fenton reaction was evaluated. pUC-19 plasmid DNA (200 ng) was incubated at 37 °C for 30 min in TE buffer (10  $\mu$ M Tris/1  $\mu$ M EDTA, pH 8.0) containing 0.35% H<sub>2</sub>O<sub>2</sub> and 50  $\mu$ M ferrous sulfate in the presence or absence of 100  $\mu$ M ochrocarpin B derivatives with a final volume of 20  $\mu$ L. DNA strand breaks induced by the Fenton reaction occurred rapidly, with most of the supercoiled pUC-19 DNA converted to the open circular form after 30 min of incubation at 37 °C. The reaction was terminated by the addition of 4  $\mu$ L of electrophoresis loading buffer (0.25% bromophenol blue and 30% glycerol).<sup>28</sup>

**4.4.4. Electron spin resonance spin trapping assay.** Inhibition of iron-induced  $\cdot$ OH formation was determined using the ESR spin trapping technique in combination with DMPO. The DMPO-OH adduct was obtained from the Fenton reaction system containing 60 mM DMPO, 2 mM H<sub>2</sub>O<sub>2</sub>, and 50  $\mu$ M ferrous ammonium sulfate with or without the test sample. This mixture was transferred to a flat quartz cell, and the ESR spectrum was measured 40 s after the addition of ferrous ammonium sulfate. The spin adducts generated in the reaction system were detected using a BRUKER spectrometer (Bruker ER070, Karlsruhe, Germany) at room temperature. Instrumental conditions were as follows: central magnetic field, 3475 G; X-band modulation frequency, 100 KHz; power, 6.4 mW; modulation amplitude, 5 G; time constant, 655.4 ms; and sweep time, 83.9 s. ESR spectra were measured at room temperature. The intensity of the DMPO-OH spin adduct was evaluated by comparing the peak height of the DMPO-OH signal.<sup>29</sup>

#### Acknowledgments

This study was supported by the National Science Council, Taiwan (NSC93-2113-M-038-004), and Taipei Medical University (TMU93-AE1-B-10).

#### References and notes

- Yu, D.; Suzuki, M.; Xie, L.; Morris-Natschke, S. L.; Lee, K. H. *Med. Res. Rev.* **2003**, *23*, 322.
- Egan, D.; O'Kennedy, R.; Moran, E.; Cox, D.; Prosser, E.; Thornes, R. D. *Drug Metab. Rev.* **1990**, *22*, 503.
- Wattenburg, L. M.; Lam, L. K. T.; Fladmoe, A. V. *Cancer Res.* **1979**, *39*, 1651.
- Feur, G.; Kellen, L. A.; Kovacs, K. *Oncology* **1976**, *33*, 35.
- Weber, U. S.; Steffen, B.; Siegers, C. P. *Res. Commun. Mol. Pathol. Pharm. Des.* **1998**, *99*, 193.
- Lorico, A.; Long, B. H. *Eur. J. Cancer A* **1993**, *29*, 1985.
- Bauer, P. I.; Kirsteen, E.; Varadi, G.; Young, L. J.; Hakam, A.; Comstock, J. A.; Kun, E. *Biochemie* **1995**, *77*, 374.
- Lee, M.; Roldan, M. C.; Haskell, M. K.; McAdam, S. R.; Hartley, J. A. *J. Med. Chem.* **1994**, *37*, 1208.
- Fylaktakidou, K. C.; Hadjipavlou-Litina, D. J.; Litnas, K. E.; Nicolaides, D. N. *Curr. Pharmaceut. Design* **2004**, *10*, 3813.

10. Lin, C. H.; Chang, C. W.; Wang, C. C.; Chang, M. S.; Yang, L. L. *J. Pharm. Pharmacol.* **2002**, *54*, 1271.
11. Murakami, A.; Nakamura, Y.; Tanaka, T.; Kawabata, K.; Takahashi, D.; Koshimizu, K.; Ohigashi, H. *Carcinogenesis* **2000**, *21*, 1843.
12. Wang, C. C.; Lai, J. E.; Chen, L. G.; Yen, K. Y.; Yang, L. L. *Bioorg. Med. Chem.* **2000**, *8*, 2701.
13. Silvan, A. M.; Abad, M. J.; Bermejo, P.; Sollhuber, M.; Villar, A. *J. Nat. Prod.* **1996**, *59*, 1183.
14. Paya, M.; Halliwell, B.; Hoult, J. R. S. *Biochem. Pharmacol.* **1992**, *44*, 205.
15. Paya, M.; Goodwin, P. A.; de las Heras, B.; Hoult, J. R. S. *Biochem. Pharmacol.* **1994**, *48*, 445.
16. Lala, P. K.; Chakraborty, C. *Lancet Oncol.* **2001**, *2*, 149.
17. Mordan, L. J.; Burnett, T. S.; Zhang, L. X.; Tom, J.; Cooney, R. V. *Carcinogenesis* **1993**, *14*, 1555.
18. Komatsu, W.; Ishihara, K.; Murata, M.; Saito, H.; Shinohara, K. *Free Radical Biol. Med.* **2003**, *34*, 1006.
19. Chaturvedula, V. S. P.; Schilling, J. K.; Kingston, D. G. I. *J. Nat. Prod.* **2002**, *65*, 965.
20. Pechmann, H. V.; Duisberg, C. *Ber.* **1883**, *16*, 2119.
21. Osborne, A. G. *Tetrahedron* **1981**, *37*, 2021.
22. Corrie, J. E. T. *J. Chem. Soc., Perkin Trans. 1* **1990**, 2151.
23. Bala, K. R.; Seshadri, T. R. *Phytochemistry* **1971**, *10*, 1131.
24. Crombie, L.; Jones, R. C. F.; Palmer, C. J. *Tetrahedron Lett.* **1985**, *26*, 2929.
25. Crombie, L.; Jones, R. C. F.; Palmer, C. J. *J. Chem. Soc., Perkin Trans. 1* **1987**, 317.
26. Lin, C. M.; Huang, S. T.; Liang, Y. C.; Lin, M. S.; Shih, C. M.; Chang, Y. C.; Chen, T. Y.; Che, C. T. *Planta Med.* **2005**, *71*, 748.
27. Huang, S. T.; Chen, C. T.; Chien, K. T.; Huang, S. H.; Chiang, B. H.; Wang, L. F.; Kuo, H. S.; Lin, C. M. *Ann. N. Y. Acad. Sci.* **2005**, *1042*, 387.
28. Lin, C. M.; Chen, C. T.; Lee, H. H.; Lin, J. K. *Planta Med.* **2002**, *68*, 363.
29. Ishikawa, S.; Yano, Y.; Arihara, K.; Itoh, M. *Biosci. Biotechnol. Biochem.* **2004**, *68*, 1324.